JOURNAL OF SOFT COMPUTING AND DATA MINING
e-ISSN: 2716-621X

JSCDM

Vol. 5 No. 2 (2024) 83-95
https://publisher.uthm.edu.my/ojs/index.php/jscdm

Brain MRI Image Classification for Tumor Detection Using Integrated Hybrid Convolutional K-Nearest Neighbor Model

Mirza Mahfuj Hossain[1], Md Mahmudul Hasan[2], Ashraful Islam[3], Norizam Sulaiman[2]*

[1] *Department of Computer Science and Engineering*
Jashore University of Science and Technology, Jashore 7408, BANGLADESH

[2] *Faculty of Electrical and Electronics Engineering Technology*
Universiti Malaysia Pahang Al-Sultan Abdullah, Pekan, Pahang 26600, MALAYSIA

[3] *Department of Electrical and Electronic Engineering*
Jashore University of Science and Technology, Jashore 7408, BANGLADESH

*Corresponding Author: norizam@umpsa.edu.my
DOI: https://doi.org/10.30880/jscdm.2024.05.02.007

Article Info

Received: 15 October 2024
Accepted: 9 December 2024
Available online: 18 December 2024

Keywords

Brain tumor detection, brain MRI, image classification, hybrid model, Otsu's thresholding

Abstract

In the field of medical image processing, brain tumor segmentation is one of the most important and challenging jobs since manual categorization by humans can lead to incorrect diagnosis and prognosis. Furthermore, it is a frustrating chore when there is a lot of data that has to be gathered. Because brain tumors have a wide range of appearances and normal tissues and tumors are similar, it is difficult to separate specific tumor areas from pictures. Keeping this in mind, a preliminary processing method for brain MRI is presented in this study that applies Otsu's Thresholding and Morphological operation. An online image dataset (consisting of 3064 slices of brain images containing samples of meningioma, glioma, and pituitary tumor types) from 233 patients with a variety of tumor sizes, positions, forms, and intensity values of images is used for the experimental investigation. Lastly, we used Convolutional Neural Networks (CNN) and K-Nearest Neighbors (KNN) in the classical classification section. The hybrid Convolutional K-Nearest Neighbors (CKNN) model was then used, which produces superior results than the conventional used models. The primary goal of this study was to use brain MRI images to identify brain tumors. This study showed significant performance with accuracy of 89.88% for the hybrid CKNN model.

1. Introduction

The early discovery of malignant regions always aids in establishing a diagnosis of an affected person, which is one of the causes of minimizing death. The image-processing approach has suddenly gathered from all quarters of the section, and the application of the image-processing mechanism has increased in recent years [1]. Medical picture capture and storage are mostly maintained in a digital environment, and knowing the essential details about it has always been a laborious and time-consuming process [2], [3]. A common medical procedure called brain magnetic resonance imaging (MRI) is used to analyze and diagnose a variety of neurological conditions, including brain tumors, sclerosis, epilepsy, and others [4]. To obtain precise and quick results, this process can be automated using a system entirely operated by machines or computers [5].

MRI is frequently used to provide and convey anatomical information, making it ideal for brain investigations [6]. It has great spatial resolution and is quite non-intrusive. One of the trickiest difficulties is segmenting brain images. However, in many computer vision and image processing applications, image segmentation is a vital task. The idea behind the segmentation procedure is to separate the image into different areas according to certain metrics so that it can be processed further [7]. When it comes to anomaly detection, surgical planning, etc., image segmentation is essential. However, noise is a key problem leading to many segmentation strategies' failure. Due to several factors, such as quantization error, transmission, or recording media, MRI pictures themselves experience multiple sounds. Additionally, there is a problem with low contrast in medical images, which makes picture segmentation challenging.

In the field of segmentation, brain imaging segmentation is a very difficult and intricate task. However, maintaining precision during the segmentation task would be extremely helpful in recognizing neurotic tissue, tumors, etc. Detection of the brain's structure via MRI is crucial to neuroscience and has numerous uses, including the study of brain development and neuroanatomical research. Therefore, most MRI pictures are employed in medical image segmentation study analysis to comprehend and do the analysis. MRI segmentation employing learning procedures and pattern recognition approaches has proven to be quite effective for studying brain images. In technical terms, the method presents a parametric model that considers certain aspects determined by the density function [8].

However, according to [9], Brain and associated nervous system cancers are the tenth largest cause of mortality, having a rate of longevity during a period of five years of 34% for men and 36% for women. Furthermore, according to the World Health Organization (WHO), around 400,000 people worldwide are affected with brain tumors, and a total of 120,000 individuals perished in the preceding year [10]. Moreover, it is anticipated that there were 86,970 newly reported instances of primary brain tumors, both malignant and non-malignant, as well as other CNS tumors, that will be diagnosed in the US in 2019 [11].

A tumor originating in the brain is created when aberrant brain cells proliferate [12]. Tumors can be classified as benign or malignant. Malignant brain tumors begin in the brain, develop more quickly, and aggressively encroach on nearby tissues. It has the potential to spread to other brain regions and impact the brain's nervous system. Primary tumors, which originate inside the brain, and secondary tumors, also referred to as brain metastasis tumors, are the two types of cancerous tumors. In contrast, a normal brain tumor is a group composed of cells that develop in the brain gradually.

Therefore, early brain tumor discovery can be crucial to increasing therapy options and the likelihood of success in surviving the tumor. However, because a lot of MRI pictures are created during ordinary medical procedures, manually segmenting tumors or lesions is a difficult, time-consuming operation. The primary uses of MRI are the detection of brain lesions and tumors. Since brain tumor segmentation from MRI typically requires an immense amount of data, it is one of the most important problems in the processing of medical imagery. Furthermore, tumors may have soft tissue boundaries and be ill-defined. Thus, obtaining a precise segmentation and accurate detection of a tumor from the human brain is a very complex task.

This work introduces a hybrid model that utilizes brain MRI scans to detect brain tumors. The hybrid model utilizes convolutional processing to identify concealed local data within brain activity, while the KNN algorithm is employed to categorize and extract characteristics. Here is a concise overview of the main contributions of the study:

- The approach suggested involves designing a hybrid model (CKNN) that combines CNN's convolutional operation with a KNN classifier. This integration aims to enhance the efficiency of brain tumor identification.
- Furthermore, the outcomes have been assessed using CNN, KNN, and CKNN models, and the suggested CKNN model exhibits superior performance in identifying brain tumors from MRI images.

The remainder of the article is organized as follows: a literature review is presented in section 2, a complete methodology is explained in section 3, and a comprehensive experimental result is explained in section 4. This section also discusses the proposed model's comparison with related studies and the significant advantages of our proposed approach over earlier studies. Section 5 concludes the outcome of the presented study.

2. Related Work

Separating the region of interest from an object is a challenging task, and isolating the tumor from an MRI brain imaging is especially challenging. Scientists worldwide are conducting research in this field to identify the most effective segmented Region of Interest (ROI) and explore various approaches from different angles. In the present era, implementing various segmentation techniques yields noteworthy outcomes, and the adoption of hybrid models is steadily growing.

Devkota et al. [13] established that the whole segmentation procedure utilizes a spatial FCM approach and Mathematical Morphological Operations, which significantly cuts down on computing time; nonetheless, the suggested approach was not tested until the assessment phase, and the findings reveal that the classifier manages

J. of Soft Computing and Data Mining Vol. 5 No. 2 (2024) p. 83-95

a success rate of 86.6%. It was similar to the Histogram-based segmentation method used by Yantao et al. [14]. The brain tumor segmentation challenge can be approached as the three-tiered classification problem, where the classes are tumor (including necrosis and tumor), edema, and normal tissue. This classification is based on two modalities, FLAIR and T1. Using the FLAIR modality, a segmentation model that uses regions to define the contours was utilized to identify the anomalous areas. The k-means method was employed to detect the swelling and tumors in the aberrant regions using the T1 modality with contrast enhancement. This methodology yielded a Dice coefficient of 73.6%.

The canny edge detecting framework utilizes customized thresholding for the purpose of extracting the ROI based on edge detection methods utilized in [15]. The set of data comprised 102 images. Images were initially processed beforehand, after which two instances of a network of neurons were applied: canny edge detection for the first set and adaptive thresholding for the second. After segmenting the image, a level number is allocated, and then typical features are retrieved using the Harris approach. Then, two neural networks are used: one for detecting healthy or tumor-containing brains and another for detecting tumor kinds. In terms of accuracy, upon comparing the outcomes of these two models, it was observed that the canny edge detection method surpassed the other model. A strategy that utilizes tumor growth patterns as new characteristics to enhance the segmentation of tumors based on texture in longitudinal MRI is introduced in [16]. Label maps are utilized for the purpose of simulating the advancement of tumors and estimating the density of cells. This is achieved by extracting various textures, such as fractal and mBm, as well as intensity attributes.

To learn vector quantization, Dina et al. [17] created a paradigm based on Neural Networks with a Probability Model. The model underwent testing on a total of 64 MRI images, with 18 of them being used as an experiment set and the remaining images used for training. The Gaussian filter smoothed out the photos. The upgraded PNN approach lowered the execution duration by 79%. Othman et al. created a segmentation algorithm based on probabilistic neural networks. Principal Component Analysis (PCA) was employed to detect characteristics and decrease the vast data dimensionality [18]. MRI images are turned into matrices, which are then classified using a Probabilistic Neural Network. Finally, the efficiency investigation was concluded. The dataset used for training had 20 participants, while the testing dataset contained 15 individuals. Based on the magnitude of the spread, accuracy fluctuated between 73 to 100%.

Rajendran et al. [19] obtained a 95.3% accuracy for the ASM and an 82.1% accuracy for the Jaccard Index utilizing the Enhanced Probabilistic Fuzzy C-Means model together with specific morphological methods. In order to segregate tumors, Zahra et al. [20] used the LinkNet network. Initially, they employed a single Linknet network to segregate seven training datasets. They ignored the image's viewpoint angle and developed a way for CNN to automatically segregate the most prevalent forms of brain tumors without requiring it for preprocessing procedures. A one-unit network achieves a Dice score of 0.73, whereas several systems earn 0.79.

Nevertheless, deep learning (DL) approaches have the potential to surpass the constraints of machine learning (ML) approaches due to their exceptional ability to acquire data [21], [22]. The presence of multiple concealed levels in the deep learning architecture allows for the transparent acquisition of hierarchical concepts. Nevertheless, despite their successful utilization in past brain tumor identification obligations, DL models still face several unresolved difficulties. Recent research like [23] – [26] has widely employed the KNN method for the purpose of brain tumor identification. Although the algorithm used in KNN has certain inherent benefits for the neuro field, most studies yielded inferior outcomes when it came to diagnosing hearing impairments. Also, before using the KNN method on any information set, features must be scaled (normalized or standardized). Otherwise, the technique can produce wrong projections. Combining multiple classifiers could serve as a viable solution to achieve flawless classification tasks, especially when individual classifiers have constraints. The investigators have developed hybrid models incorporating multiple techniques to achieve this objective.

In studies [27], [28], hybrid algorithms were employed, effectively combining the strengths of multiple designs. This integration resulted in enhanced performance and greater efficacy compared to using a single classifier in specific scenarios, demonstrating the potential benefits of hybrid approaches in improving classification outcomes. Khairandish et al. [29] implemented a hybrid CNN-SVM model for the detection of brain tumors using MRI scans, demonstrating the effectiveness of combining convolutional neural networks with support vector machines for improved accuracy in tumor identification. In a similar vein, another study [30] introduced a hybrid CNN-DWA model, which not only detects brain tumors from MRI images but also classifies them into different categories. These studies highlight the potential of hybrid deep learning models in enhancing the precision and reliability of brain tumor diagnosis from medical imaging.

3. Methods

The suggested approach is designed to precisely identify and categorize normal and abnormal MRIs. Figure 1 depicts the entire method employed in this study, which first reads the brain MRI and applies preprocessing. The MRI images are then processed to determine whether they are normal or aberrant using three distinct classification models.

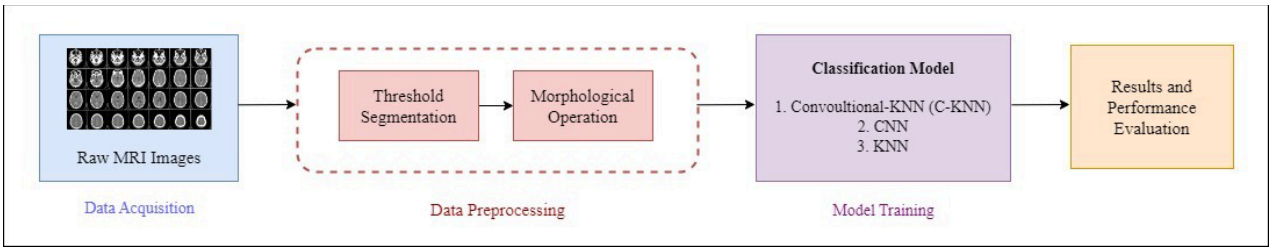

Fig. 1 *Comprehensive methodology of the proposed investigation*

3.1 Data Description

The dataset consists of 3064 slices of brain T1-weighted Contrast Enhanced-MRI (CE-MRI) scans from 233 different people. This contains 708 meningiomas, 1426 gliomas, and 930 pituitary tumors, which are freely accessible [31] and are used in this experiment. In clinical settings, only a limited number of brain CE-MRI slices with a substantial slice gap are typically recorded and made reachable rather than a full 3D volume. Creating a 3D model with such scant data is tough. Thus, the suggested technique relies on 2-dimensional sections. The brain T1-weighted CE-MRI dataset was acquired from Nanfang Hospital in Guangzhou, China, and General Hospital at Tianjin Medical University in China over the period of 2005 to 2010. The pictures have a spatial resolution of 512×512 pixels and a pixel size of 0.49×0.49 mm^2. The thickness of each slice is 6 mm, while there is a space of 1 mm between each slice. Three proficient radiologists meticulously delineated the tumor boundaries. Additional details regarding this dataset can be acquired by referring to the sources cited in the range of [32], [33].

3.2 Data Preprocessing

The raw MRI images were subjected to image preprocessing methods to remove unwanted disturbances and artifacts. Preprocessing consists of several procedures. First, the input picture matches a reference image in the registration process. The skull and other undesired elements have been eliminated from the input registered picture. Otsu's thresholding is extensively employed for binarizing grayscale images, particularly in cases where there is a significant contrast between object and background intensities [34]. Moreover, morphological operations are widely utilized for applications such as edge detection, noise reduction, image enhancement, and object segmentation [35]. Therefore, this study employs Otsu's thresholding and morphological operations as preprocessing techniques to enhance images and accurately identify tumor boundaries.

3.2.1 Otsu's Thresholding

For skull removal, we initially employed Otsu's Thresholding approach, which determines the threshold value and divides the picture into the backdrop and the forefront. This technique involves selecting a threshold that decreases the variability within each class. Intra-class variance is defined as the sum of weighted variances between the two classes.

Otsu's technique uses interclass variance as a statistic to evaluate a threshold. The ideal threshold value is the one that maximizes the interclass variation. Consider $f(x, y)$ as a grayscale snap with individual pixel intensity spanning between 0 to L - 1, where L indicates the entire quantity of unique intensity levels and the variable n_i signifies the total count of pixels that have a gray level quantity equivalent to "i", then $N = \sum_{i=0}^{L-1} n_i$ adds up all the pixels across the whole picture. If p_i indicates the chance of a pixel having a grey level value i, it is possible to estimate in practice using the frequency described as $p_i = \frac{n_i}{N}$. By setting the threshold value to T, we may divide the pixels of the picture into two classes, namely C_0 and C_1, for a binary segmentation task, where the two sets of pixels, C_0 and C_1, comprise pixels with grey values ranging from [0, T] and [T + 1, L - 1] respectively. Prior to providing the concept of interclass variances, it is necessary to introduce many significant statistics. These include the average pixel grey value of C_0 and C_1, as well as the weight parameters, which are represented by distinct signs $\mu_0(T)$, $\mu_1(T)$, $\omega_0(T)$ and $\omega_1(T)$. The following Equations (1) to (3) is a definition of the aforementioned measurements, a detailed explanation of these equations can be found in [36].

$$\mu_0(T) = \frac{\sum_{i=0}^{T} i p_i}{\omega 0\,(T)}, \quad \omega_0(T) = \sum_{i=0}^{T} p_i \tag{1}$$

$$\mu_1(T) = \frac{\sum_{i=T+1}^{L} i p_i}{\omega 1\,(T)}, \quad \omega_1(T) = \sum_{i=T+1}^{L} p_i \tag{2}$$

$$\mu = \frac{\sum_{i=0}^{L} ip_i}{\sum_{i=0}^{L} p_i} = \sum_{i=0}^{L} ip_i = \omega_0(T).\mu_0(T) + \omega_1(T).\mu_1(T) \quad (3)$$

The grey value projections for C_0 and C_1 are denoted as $\mu_0(T)$ and $\mu_1(T)$, respectively, in Equations (1) to (3), where μ represents the average grey value of all pixel values in the entire picture. Equation (4) can be used to describe the interclass variance of C_0 and C_1 given the preceding definitions as $\sigma_B(T)$, where T is the segmented threshold.

$$\sigma_B(T) = \omega 0(T)(\mu 0(T) - \mu)^2 + \omega 1(T)(\mu 1(T) - \mu)^2 \quad (4)$$

In Equation (4), there are two components that make up the interclass variance. These components represent the two classes C_0 and C_1, which are described in (1) and (2), and have different weights $\omega_0(T)$ and $\omega_1(T)$ respectively. Once the variation across classes $\sigma_B(T)$ of C_0 and C_1 achieves its maximum value when employing T^* as the threshold value, Otsu's method considers the gray value T^* as the ideal threshold, as mentioned earlier. Addressing the optimization challenge stated in Equation (5) is one way to express the ideal threshold value T^*.

$$T^* = arg_T \ max \ (\sigma_B \ (T)) \quad (5)$$

Due to the small size of the solution space for the aforementioned optimization problem (the range of possible grey values is [0, L—1]), the exhaust approach can be used to determine the ideal threshold T* by testing all possible gray values T. The Otsu approach works well with many real-world photos. Figure 2 shows Otsu's threshold segmentation in raw MRI images.

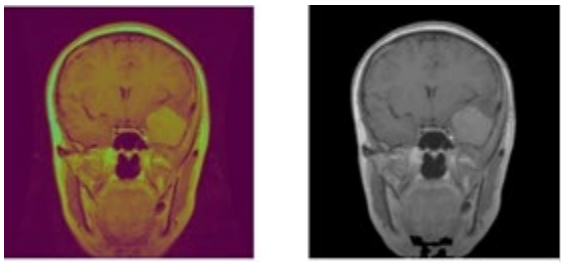

(a) **(b)**

Fig. 2 *Brain MRI image (a) Normal MRI image; (b) After Otsu's Threshold segmentation*

3.2.2 Morphological Operation

Binary images can contain various imperfections. Under specific circumstances, the presence of noise and textures can cause the distortion or collapse of binary zones that were established through basic thresholding. Morphology encompasses a wide range of image processing techniques that alter images based on their shape. It is regarded being among the data processing techniques effective in image processing. It has several uses, including texture analysis, noise removal, boundary extraction etc. [37]. Morphological image processing seeks to remove any flaws while preserving the fundamental composition of the image. In morphological processes, the numerical representations of pixels are completely disregarded in favor of their relative arrangement. As a result, they are primarily used for binary images. However, they are versatile enough to grayscale images where the exact pixel values are not considered due to unsolved light functions during image transfer.

Morphological approaches validate the picture using a tiny template known as a structural element. This structural element is applied to all feasible spots in the input picture, resulting in output of identical dimensions. In this approach, the output picture pixel values are calculated using pixels from the input image that are comparable to their neighbors. This operation generates a new digital image that, if the experiment succeeded, has a non-zero pixel value at the specified position in the input picture. There are a variety of structure components, such as diamond, square, and cross shapes. Figure 3 illustrates the before and after scenario of morphological operation of a brain MRI image.

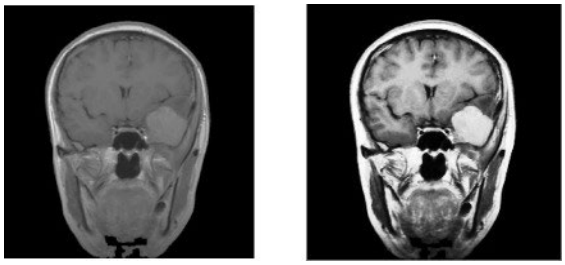

(a) (b)

Fig. 3 *Brain MRI image (a) Before morphological operation; (b) After morphological operation*

3.3 Classification Model

This work successfully combined two techniques to create the proposed CKNN model, boosting efficiency for identifying brain tumors using MRI images. Furthermore, this study used two conventional models to evaluate the performance of the proposed hybrid model compared to traditional models.

3.3.1 Proposed Hybrid CKNN Model

The created CKNN model consists of two convolution layers of data and a KNN classifier. The convolutional layers consist of various kernel sizes, pooling layers, and one dropout layer.

The convolution stage is a crucial component of CNN, providing the purpose of maintaining the link amongst images by acquiring knowledge of visual properties from small squares of input information. Convolution is a procedure where the input is multiplied by weights. This layer performs the dot product operation on a pair of matrices. One of the matrices holds the parameters that can be known as the kernel, while the other matrix holds the limited part of the field that is receptive. A statistical operation, such as image matrix manipulation, necessitates a pair of inputs: an image matrix and a filter or kernel. The measurement of the image matrix is represented as $(h \times w \times d)$, and it changes to $(f_h \times f_w \times d)$ once the filter is applied. The matrix has a final dimension of $(h - f_h + 1) \times (w - f_w + 1) \times 1$.

Every filter across the whole picture is applied using the same weight and bias settings. The weight-sharing approach is utilized to convey the entire picture with uniform characteristics. Equations (6) and (7) illustrate the l-layer complex feature maps when applied to a CNN architecture with l layers.

$$y_{l,j}^{conv} = \sum_{i}^{k} W_{i,j}^{l} * y_{l-1,i}^{pool} + b_j^l \tag{6}$$

$$y_{l,j}^{relu} = \max\left[0, y_{l-1,j}^{conv}\right] \tag{7}$$

The expression $\boldsymbol{y_{l,j}^{conv}}$ denotes the result obtained from the l-th layer, W^l denotes the kernel utilized in that layer, k signifies the quantity of kernels, b^l indicates the bias, and $f(\cdot)$ is the function that is responsible for converting the input into the output map in order to enhance the irregular characteristic. An often used alternative to the function of sigmoid activation is the rectified linear unit (relu), which is represented as max $(0, x)$. This study employed the relu function, which demonstrated superior results in the majority of tasks related to classification. It facilitated quicker convergence and mitigated the issue of the diminishing gradients [38].

The KNN method is a machine learning technique that assigns a piece of information to a certain class according to a large percentage of its neighboring data points [39]. The KNN algorithm operates in two stages: firstly, it identifies the closest neighbor's value, and subsequently, it assigns the information point to a particular group based on the value of the neighbor that is closest to it. K in KNN represents the quantity of closest neighbors. The behavior of KNN method is mostly influenced by the value of the parameter k, which represents the number of neighbors considered. One drawback of the KNN approach is its difficulty in calculating the optimal value of k. Despite many research efforts on the matter, the task of choosing the k value for the k-NN algorithm remains arduous and complicated [40]. This approach computes the distance between the samples using distance metrics Euclidean.

The Euclidean distance is the measure of the straight line joining the two occurrences. The value is calculated by taking the square of the distinction between the x and y coordinates of the points. Let A = $(A_1, A_2, \ldots, A_n)$ and B = $(B_1, B_2, \ldots\ldots, B_n)$ be two points in Euclidean n-space. The distance from A to B can be computed using Equation (8).

J. of Soft Computing and Data Mining Vol. 5 No. 2 (2024) p. 83-95

$$E.D.: (A, B) = \sqrt{\sum_{i=1}^{n} (A_i - B_i)^2} \quad (8)$$

The proposed hybrid architecture building procedure is illustrated step-by-step in Figure 4. A schematic representation of the proposed CKNN model is depicted in Figure 5. The picture represents a convolutional neural network (CNN) designed to identify MRI images. The caption of the picture indicates that the model accepts a 3D input image of size 3 x 224 x 224, which follows processing through numerous convolutional layers.

The model is structured with a series of convolutional and pooling layers for feature extraction, followed by a classification segment. It begins with an input layer that processes RGB images through two convolutional layers. The first convolutional layer consists of 32 filters with a kernel size of 6, a stride of 2, and padding of 2, followed by batch normalization, relu activation, and max pooling. The second convolutional layer comprises 64 filters with a kernel size of 4, a stride of 2, and padding of 2, followed by batch normalization, relu activation, and max pooling, using a larger 3x3 pooling window.

Following the convolutional phase, the model flattens the output and passes it to a fully connected linear layer, producing a 128-dimensional feature vector. This is followed by dropout regularization, and the process concludes with an output layer corresponding to the desired number of classes. Weight decay is applied to both the convolutional and linear layers to mitigate overfitting. Instead of using the fully connected layers for classification, the model's flattened feature vector is input into a KNN algorithm. This approach leverages CNN's feature extraction capabilities while utilizing KNN for classification, combining the strengths of CNN for feature learning with the simplicity of KNN for classification.

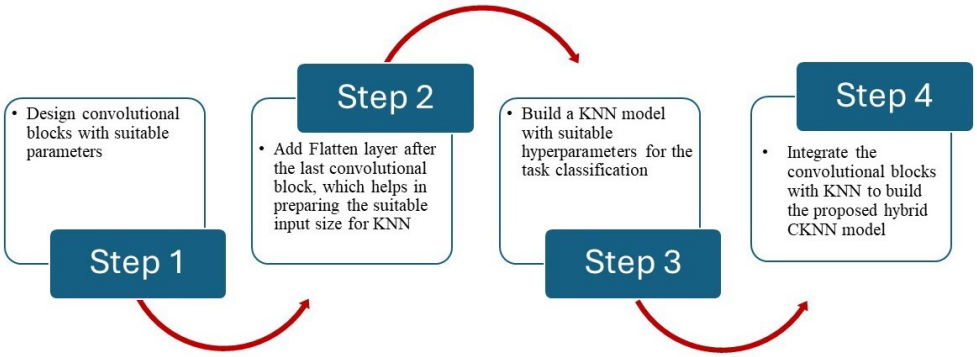

Fig. 4 *Hybrid model building procedure*

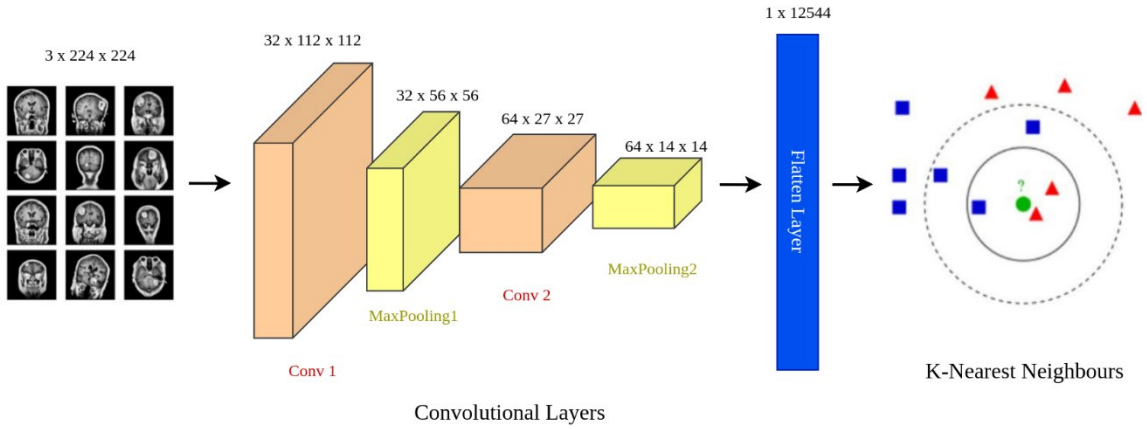

Fig. 5 *Schematic diagram of proposed CKNN model*

However, this experimental investigation was conducted in Python with the assistance of Ubuntu 20.04, Ryzen-5 2500U @ 2.50GHz, GTX 1030, and CUDA Version 12.

3.4 Performance Evaluation

A variety of measures are used to evaluate classifier performance and outcomes of classification in order to determine the excellence of the classification. These measurements consist of Cohen's Kappa, F1-score, recall, precision, and accuracy of categorization.

$$Accuracy = \frac{TP+TN}{TP+FN+TN+FP} \; x\; 100\% \tag{9}$$

The classifier's accuracy in correctly classifying positive samples as positive and negative samples as negative throughout the whole dataset is referred to as precision [41].

$$Precision = \frac{TP}{TP+FP} \; x\; 100\% \tag{10}$$

The percentage of positive samples that are accurately recognized is shown by the recall value.

$$Recall = \frac{TP}{TP+FN} \; x\; 100\% \tag{11}$$

Where TP, TN, FP, and FN depict the semantics of true positive, true negative, false positive, and false negative, respectively.

The weighted average of accuracy and recall, with the greatest values at 1 and the poorest values at 0, is known as the F1-score [42].

$$F1 = \frac{2*Precision*Recall}{Precision+Recall} \; x\; 100\% \tag{12}$$

A statistical metric called Cohen's kappa is used to evaluate the reliability or inter-rater agreement of categorical items. The concurrence between two raters that goes above and beyond what would be predicted by chance alone is measured by Cohen's kappa statistic. The Cohen's Kappa evaluation level is shown in Table 1.

Table 1 *Evaluation criterion of Cohen's Kappa*

Value of Cohen's Kappa	Level of agreement
≤ 0	No agreement
0.01 – 0.20	None to slight
0.21 – 0.40	Fair
0.41 – 0.60	Moderate
0.61 – 0.80	Substantial
0.81 – 1.00	Almost perfect agreement

4. Result and Discussion

Using the dataset of MRI scans that is accessible to the public, an experiment is conducted to evaluate the effectiveness of the model. This study has used three different models to evaluate how well brain MRI pictures can detect tumors.

4.1 Experimental Result of the Models

The KNN, CNN, and hybrid CKNN models have all been used in this investigation. The comparison of three applied models' accuracies in terms of brain tumor identification from MRI images is shown in Figure 6.

J. of Soft Computing and Data Mining Vol. 5 No. 2 (2024) p. 83-95

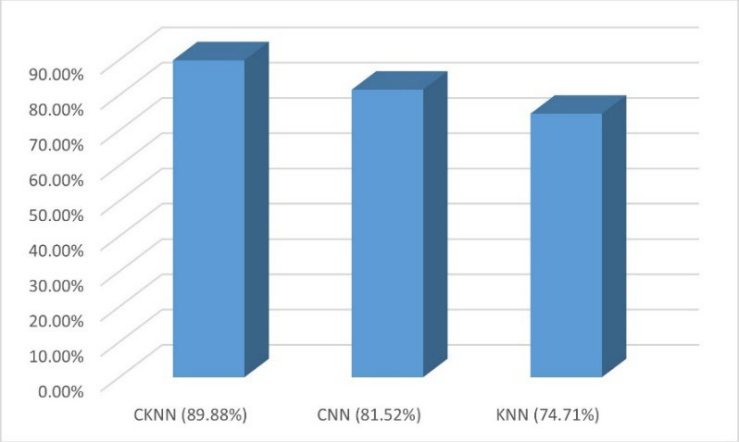

Fig. 6 *Accuracy comparison among three applied models*

Table 2 compares the three models' performance in brain tumor identification and highlights differences between the performance of the provided model and the other two models. The precision, recall, F1-score, and Cohen's kappa score for the experimental analysis using the KNN model are 90.27%, 74.70%, 81.09%, and 0.57, respectively. An output of 81.12% precision, 81.52% recall, 80.89% F1-score, and 0.71 Cohen's kappa score are obtained for the analysis using the CNN model.

Table 2 *Different performance metrices of applied three models*

Method	Precision	Recall	F1-Score	Cohen's Kappa
KNN	90.27%	74.70%	81.09%	0.57
CNN	81.12%	81.52%	80.89%	0.71
Proposed CKNN	90.57%	89.89%	90.12%	0.84

The precision, recall, F1-score, and Cohen's kappa score for the suggested CKNN model are 90.57%, 89.89%, 90.12%, and 0.84, respectively. The analysis result shows that the proposed CKNN model outperformed the KNN model by 15.17% in terms of accuracy, 0.30% precision, 15.19% recall, and 9.03% F1-Score improvement; in comparison, the CNN model outperformed the proposed CKNN model by 8.36%, 9.45% precision, 8.37% recall, and 9.23% F1-Score improvement.

However, confusion matrices are quite useful in machine learning since they are great instruments for characterizing a classification model's performance. True positives, true negatives, false positives, and false negatives are the four distinct categories into which predictions can be divided in order to assess the accuracy of the model. The previously mentioned data is essential for evaluating the benefits and limitations of the model, identifying possible areas for improvement, and fine-tuning algorithms to maximize its overall efficiency.

As Figure 7 illustrates, all models perform satisfactorily when it comes to True Negatives. However, the results show that the CKNN model performs best overall, particularly when it comes to correctly identifying positive scenarios and maintaining a low proportion of false positives. It is, hence, the standout choice among the applicable models.

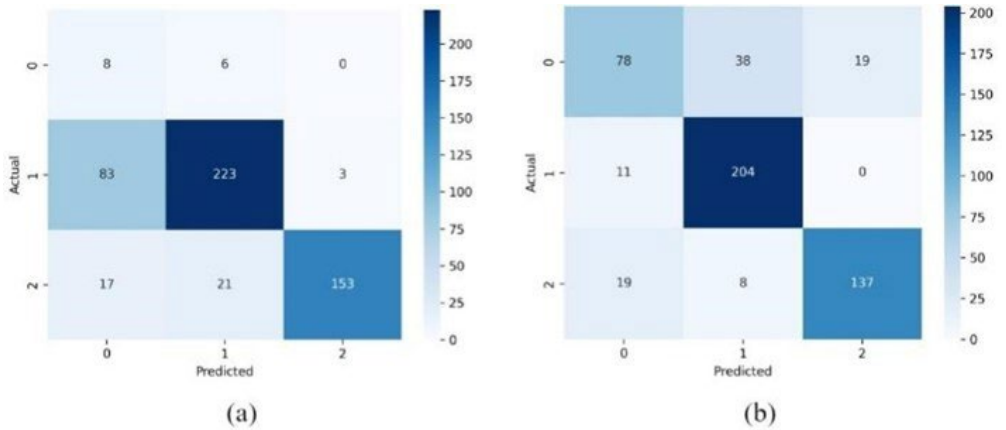

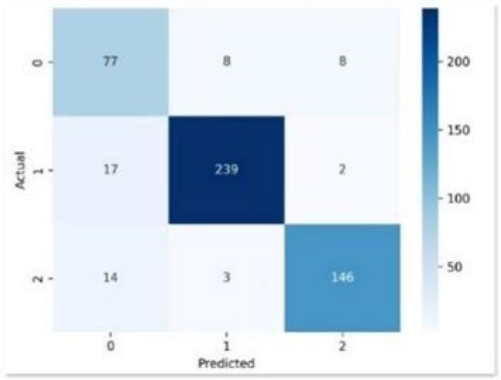

(c)

Fig. 7 *Confusion Matrix (a) KNN; (b) CNN; (c) CKNN model*

4.2 Performance Comparison with Related Studies

Due to advancements in computer technology, the use of ML and DL algorithms has significantly increased in the past few years in the identification of hearing loss. Various ML and DL methods have also been employed to identify brain cancers at an early stage. Table 3 presents the differences between the proposed approach and the related studies.

Table 3 *Performance comparison with related studies*

Reference	Imaging Modality	Processing Technique	Classification Model	Result	Drawback
[43]	T1-CE	Normalization between -1 to 1 Data augment (rotate + mirror)	CNN-GAN	88%	Complicated procedure. Absence of comparisons.
[44]	MRI images	Glioma segmentation	Deep CNN and SVM	CNN 86.69% and SVM 87.05%	The model isn't optimized.
[13]	MRI images	Morphological reconstruction	SVM	86.6%	Not undergone testing till the evaluation phase.
[45]	MRI images	Wiener filter and contrast limited adaptive histogram equalization (CLAHE)	Neural network and SVM	85.4%	The intricacy of earlier segmentation.
[46]	T1-CE	Normalized using minmax method	F-RCNN and region proposal uses VGG-16 as the base network	Average precision of 75.18% for glioma, 89.45% for meningioma and 68.18% for pituitary tumor	The concept of testing time is not explained. The intricacy of the region proposal network.

Proposed CKNN model	MRI images	Otsu's threshold and morphological operation	Hybrid CKNN	89.88%

Although the suggested hybrid approach outperforms standard machine learning and deep learning methods in detecting brain cancers from MRI images, it possesses a few limitations. The restricted range of dataset sizes impedes the efficacy of this investigation. Additional research is required to assess the efficacy of the suggested method on large-scale 3D image datasets. In our forthcoming research, we will delve more into the intricacies of multi-parameter adaptation.

5. Conclusion

This research presents a method for distinguishing between brain tumors and normal MRI pictures. The system reads the brain MRI, after which it preprocesses and categorizes the results. Otsu's threshold segmentation and morphological operation are performed on the MRI images during preprocessing. The photos are then classified as normal or malignant by applying these attributes. We used KNN in the conventional machine learning classifier section, which yields an accuracy of 74.71%. Subsequently, we used CNN as a conventional deep learning classifier, yielding an 81.52% accuracy. In addition, we employed a hybrid CKNN model for improved outcomes, yielding an accuracy of 89.88%. To obtain more effective brain tumor segmentation, we intend to work with 3D brain imaging in the future. This element of dealing with an expanded dataset will provide more challenges; thus, in order to speed up the breadth of our work, we want to construct a dataset that emphasizes abridgment.

Acknowledgement

The authors would like to thank the owner of the dataset for making the dataset publicly available.

Conflict of Interest

Authors declare that there is no conflict of interests regarding the publication of the paper.

Author Contribution

The authors confirm their contribution to the paper as follows: ***study conception and design:*** *Mirza Mahfuj Hossain, Md Mahmudul Hasan;* ***analysis and interpretation of results:*** *Mirza Mahfuj Hossain;* ***draft manuscript preparation:*** *Md Mahmudul Hasan, Ashraful Islam, Norizam Sulaiman. All authors reviewed the results and approved the final version of the manuscript.*

References

[1] Ker, J., Wang, L., Rao, J., & Lim, T. (2018). Deep Learning Applications in Medical Image Analysis. IEEE Access, 6, 9375–9389. https://doi.org/10.1109/ACCESS.2017.2788044

[2] Zhou, T., Ruan, S., & Canu, S. (2019). A review: Deep learning for medical image segmentation using multi-modality fusion. *Array*, *3–4*, 100004. https://doi.org/10.1016/j.array.2019.100004

[3] Jaglan, P., Dass, R., & Duhan, M. (2019). A Comparative Analysis of Various Image Segmentation Techniques. In C. R. Krishna, M. Dutta, & R. Kumar (Eds.), *Proceedings of 2nd International Conference on Communication, Computing and Networking* (Vol. 46, pp. 359–374). Springer Singapore. https://doi.org/10.1007/978-981-13-1217-5_36

[4] Sathya, A., Senthil, S., & Samuel, A. (2012). Segmentation of breast MRI using effective Fuzzy C-Means method based on Support Vector Machine. *2012 World Congress on Information and Communication Technologies*, 67–72. https://doi.org/10.1109/WICT.2012.6409052

[5] Singh, M., Verma, A., & Sharma, N. (2018). An Optimized Cascaded Stochastic Resonance for the Enhancement of Brain MRI. *IRBM*, *39*(5), 334–342. https://doi.org/10.1016/j.irbm.2018.08.002

[6] Kumar Mallick, P., Ryu, S. H., Satapathy, S. K., Mishra, S., Nguyen, G. N., & Tiwari, P. (2019). Brain MRI Image Classification for Cancer Detection Using Deep Wavelet Autoencoder-Based Deep Neural Network. *IEEE Access*, *7*, 46278–46287. https://doi.org/10.1109/ACCESS.2019.2902252

[7] Pham, T. X., Siarry, P., & Oulhadj, H. (2018). Integrating fuzzy entropy clustering with an improved PSO for MRI brain image segmentation. *Applied Soft Computing*, *65*, 230–242. https://doi.org/10.1016/j.asoc.2018.01.003

[8] Tong, J., Zhao, Y., Zhang, P., Chen, L., & Jiang, L. (2019). MRI brain tumor segmentation based on texture features and kernel sparse coding. *Biomedical Signal Processing and Control*, *47*, 387–392. https://doi.org/10.1016/j.bspc.2018.06.001

[9] Brain Tumor: Statistics, Cancer.Net Editorial Board, 11/2017 (accessed on 05.04.2024)
[10] Rajasekaran, K. A., & Gounder, C. C. (2018). Advanced Brain Tumour Segmentation from MRI Images. In A. M. Halefoğlu (Ed.), *High-Resolution Neuroimaging—Basic Physical Principles and Clinical Applications*. InTech. https://doi.org/10.5772/intechopen.71416
[11] General Information About Adult Brain Tumors. NCI. 14 April 2014. (accessed on 11.05.2019)
[12] Hossain, T., Shishir, F. S., Ashraf, M., Al Nasim, M. A., & Muhammad Shah, F. (2019). Brain Tumor Detection Using Convolutional Neural Network. *2019 1st International Conference on Advances in Science, Engineering and Robotics Technology (ICASERT)*, 1–6. https://doi.org/10.1109/ICASERT.2019.8934561
[13] Devkota, B., Alsadoon, A., Prasad, P. W. C., Singh, A. K., & Elchouemi, A. (2018). Image Segmentation for Early Stage Brain Tumor Detection using Mathematical Morphological Reconstruction. *Procedia Computer Science*, *125*, 115–123. https://doi.org/10.1016/j.procs.2017.12.017
[14] Song, Y., Ji, Z., Sun, Q., & Zheng, Y. (2017). A Novel Brain Tumor Segmentation from Multi-Modality MRI via A Level-Set-Based Model. *Journal of Signal Processing Systems*, *87*(2), 249–257. https://doi.org/10.1007/s11265-016-1188-4
[15] Badran, E. F., Mahmoud, E. G., & Hamdy, N. (2010). An algorithm for detecting brain tumors in MRI images. *The 2010 International Conference on Computer Engineering & Systems*, 368–373. https://doi.org/10.1109/ICCES.2010.5674887
[16] Pei, L., Reza, S. M. S., Li, W., Davatzikos, C., & Iftekharuddin, K. M. (2017). *Improved brain tumor segmentation by utilizing tumor growth model in longitudinal brain MRI* (S. G. Armato & N. A. Petrick, Eds.; p. 101342L). https://doi.org/10.1117/12.2254034
[17] Dahab, D. M. A., Ghoniemy, S., & Selim, G. (2012). Automated Brain Tumor Detection and Identification Using Image Processing and Probabilistic Neural Network Techniques. *International Journal of Image Processing and Visual Communication*, 1–8.
[18] Othman, M. F., & Basri, M. A. M. (2011). Probabilistic Neural Network for Brain Tumor Classification. *2011 Second International Conference on Intelligent Systems, Modelling and Simulation*, 136–138. https://doi.org/10.1109/ISMS.2011.32
[19] Rajendran, A., & Dhanasekaran, R. (2012). Fuzzy Clustering and Deformable Model for Tumor Segmentation on MRI Brain Image: A Combined Approach. *Procedia Engineering*, *30*, 327–333. https://doi.org/10.1016/j.proeng.2012.01.868
[20] Sobhaninia, Z., Rezaei, S., Noroozi, A., Ahmadi, M., Zarrabi, H., Karimi, N., Emami, A., & Samavi, S. (2018). *Brain Tumor Segmentation Using Deep Learning by Type Specific Sorting of Images* (arXiv:1809.07786). arXiv. http://arxiv.org/abs/1809.07786
[21] Mohsen, H., El-Dahshan, E.-S. A., El-Horbaty, E.-S. M., & Salem, A.-B. M. (2018). Classification using deep learning neural networks for brain tumors. *Future Computing and Informatics Journal*, *3*(1), 68–71. https://doi.org/10.1016/j.fcij.2017.12.001
[22] Nossier, S. A., Rizk, M. R. M., Moussa, N. D., & El Shehaby, S. (2019). Enhanced smart hearing aid using deep neural networks. *Alexandria Engineering Journal*, *58*(2), 539–550. https://doi.org/10.1016/j.aej.2019.05.006
[23] Ramdlon, R. H., Martiana Kusumaningtyas, E., & Karlita, T. (2019). Brain Tumor Classification Using MRI Images with K-Nearest Neighbor Method. *2019 International Electronics Symposium (IES)*, 660–667. https://doi.org/10.1109/ELECSYM.2019.8901560
[24] Saeed, S., Abdullah, A., Jhanjhi, N. Z., Naqvi, M., & Nayyar, A. (2022). New techniques for efficiently k-NN algorithm for brain tumor detection. *Multimedia Tools and Applications*, *81*(13), 18595–18616. https://doi.org/10.1007/s11042-022-12271-x
[25] Saeed, S., Abdullah, A., Jhanjhi, N. Z., Naqvi, M., & Nayyar, A. (2022). New techniques for efficiently k-NN algorithm for brain tumor detection. Multimedia Tools and Applications, 81(13), 18595–18616. https://doi.org/10.1007/s11042-022-12271-x
[26] Angel Viji, K. S., & Hevin Rajesh, D. (2020). An Efficient Technique to Segment the Tumor and Abnormality Detection in the Brain MRI Images Using KNN Classifier. Materials Today: Proceedings, 24, 1944–1954. https://doi.org/10.1016/j.matpr.2020.03.622
[27] Islam, M. S., Islam, M. N., Hashim, N., Rashid, M., Bari, B. S., & Farid, F. A. (2022). New Hybrid Deep Learning Approach Using BiGRU-BiLSTM and Multilayered Dilated CNN to Detect Arrhythmia. IEEE Access, 10, 58081–58096. https://doi.org/10.1109/ACCESS.2022.3178710
[28] Wu, H., Gurram, P., Kwon, H., & Prasad, S. (2014). A hybrid CSVM-HMM model for acoustic signal classification using a tetrahedral sensor array. *IEEE SENSORS 2014 Proceedings*, 1352–1355. https://doi.org/10.1109/ICSENS.2014.6985262
[29] Khairandish, M. O., Sharma, M., Jain, V., Chatterjee, J. M., & Jhanjhi, N. Z. (2022). A Hybrid CNN-SVM Threshold Segmentation Approach for Tumor Detection and Classification of MRI Brain Images. IRBM, 43(4), 290–299. https://doi.org/10.1016/j.irbm.2021.06.003

[30] El Kader, I. A., Xu, G., Shuai, Z., & Saminu, S. (2021). Brain Tumor Detection and Classification by Hybrid CNN-DWA Model Using MR Images. Current Medical Imaging Formerly Current Medical Imaging Reviews, 17(10), 1248–1255. https://doi.org/10.2174/1573405617666210224113315
[31] KAVI, D. (2021). *Brain Tumor Image Dataset*. https://www.kaggle.com/datasets/denizkavi1/brain-tumor
[32] Cheng, J., Huang, W., Cao, S., Yang, R., Yang, W., Yun, Z., Wang, Z., & Feng, Q. (2015). Enhanced Performance of Brain Tumor Classification via Tumor Region Augmentation and Partition. *PLOS ONE*, *10*(10), e0140381. https://doi.org/10.1371/journal.pone.0140381
[33] Cheng, J., Yang, W., Huang, M., Huang, W., Jiang, J., Zhou, Y., Yang, R., Zhao, J., Feng, Y., Feng, Q., & Chen, W. (2016). Retrieval of Brain Tumors by Adaptive Spatial Pooling and Fisher Vector Representation. *PLOS ONE*, *11*(6), e0157112. https://doi.org/10.1371/journal.pone.0157112
[34] Feng, Y., Zhao, H., Li, X., Zhang, X., & Li, H. (2017). A multi-scale 3D Otsu thresholding algorithm for medical image segmentation. Digital Signal Processing, 60, 186–199. https://doi.org/10.1016/j.dsp.2016.08.003
[35] Sheela, C. J. J., & Suganthi, G. (2020). Morphological edge detection and brain tumor segmentation in Magnetic Resonance (MR) images based on region growing and performance evaluation of modified Fuzzy C-Means (FCM) algorithm. Multimedia Tools and Applications, 79(25–26), 17483–17496. https://doi.org/10.1007/s11042-020-08636-9
[36] Yang, P., Song, W., Zhao, X., Zheng, R., & Qingge, L. (2020). An improved Otsu threshold segmentation algorithm. International Journal of Computational Science and Engineering, 22(1), 146. https://doi.org/10.1504/IJCSE.2020.107266
[37] Chudasama, D., Patel, T., Joshi, S., & I. Prajapati, G. (2015). Image Segmentation using Morphological Operations. *International Journal of Computer Applications*, *117*(18), 16–19. https://doi.org/10.5120/20654-3197
[38] Krizhevsky, A., Sutskever, I., & Hinton, G. E. (2017). ImageNet classification with deep convolutional neural networks. *Communications of the ACM*, *60*(6), 84–90. https://doi.org/10.1145/3065386
[39] Islam, M. N., Sulaiman, N., Bari, B. S., Rashid, M., & Mustafa, M. (2022). A hybrid scheme for AEP based hearing deficiency diagnosis: CWT and convoluted k-nearest neighbour (CKNN) pipeline. *Neuroscience Informatics*, *2*(1), 100037. https://doi.org/10.1016/j.neuri.2021.100037
[40] Kang, P., & Cho, S. (2008). Locally linear reconstruction for instance-based learning. *Pattern Recognition*, *41*(11), 3507–3518. https://doi.org/10.1016/j.patcog.2008.04.009
[41] Hasan, M. M., Khandaker, S., Sulaiman, N., Mahfuj Hossain, M., & Islam, A. (2024). Addressing Imbalanced EEG Data for Improved Microsleep Detection: An ADASYN, FFT and LDA-Based Approach. Diyala Journal of Engineering Sciences, 45–57. https://doi.org/10.24237/djes.2024.17304
[42] Hasan, M. M., Mirza, M. H., & Sulaiman, N. (2023). Fatigue State Detection Through Multiple Machine Learning Classifiers Using EEG Signal. Applications of Modelling and Simulation, 7, 178–189.
[43] Ghassemi, N., Shoeibi, A., & Rouhani, M. (2020). Deep neural network with generative adversarial networks pre-training for brain tumor classification based on MR images. *Biomedical Signal Processing and Control*, *57*, 101678. https://doi.org/10.1016/j.bspc.2019.101678
[44] Wu, W., Li, D., Du, J., Gao, X., Gu, W., Zhao, F., Feng, X., & Yan, H. (2020). An Intelligent Diagnosis Method of Brain MRI Tumor Segmentation Using Deep Convolutional Neural Network and SVM Algorithm. *Computational and Mathematical Methods in Medicine*, *2020*, 1–10. https://doi.org/10.1155/2020/6789306
[45] Natteshan, N. V. S., & Angel Arul Jothi, J. (2015). Automatic Classification of Brain MRI Images Using SVM and Neural Network Classifiers. In E.-S. M. El-Alfy, S. M. Thampi, H. Takagi, S. Piramuthu, & T. Hanne (Eds.), *Advances in Intelligent Informatics* (Vol. 320, pp. 19–30). Springer International Publishing. https://doi.org/10.1007/978-3-319-11218-3_3
[46] Bhanothu, Y., Kamalakannan, A., & Rajamanickam, G. (2020). Detection and Classification of Brain Tumor in MRI Images using Deep Convolutional Network. *2020 6th International Conference on Advanced Computing and Communication Systems (ICACCS)*, 248–252. https://doi.org/10.1109/ICACCS48705.2020.9074375